

Current-induced switching of magnetic tunnel junctions: Effects of field-like spin-transfer torque, pinned-layer magnetization orientation and temperature

R. K. Tiwari,¹ M. H. Jhon,¹ N. Ng,¹ D. J. Srolovitz,² and Chee Kwan Gan^{1,*}

¹*Institute of High Performance Computing, Agency for Science, Technology and Research, 1 Fusionopolis Way, #16-16 Connexis, Singapore 138632*

²*Department of Materials Science and Engineering, Department of Mechanical Engineering and Applied Mechanics, University of Pennsylvania, Philadelphia, PA 19104, United States*

(Dated: 12 December 2013)

We study current-induced switching in magnetic tunnel junctions (MTJs) in the presence of a field-like spin-transfer torque and tilted pinned-layer magnetization in the high current limit at finite temperature. We consider both the Slonczewski and field-like torques with coefficients a_J and b_J , respectively. At finite temperatures, $\sigma = b_J/a_J = \pm 1$ leads to a smaller mean switching time compared that with $\sigma = 0$. The reduction of switching time in the presence of the field-like term is due to the alignment effect (for $\sigma > 0$) and the initial torque effect.

PACS numbers:

Keywords: Spin transfer torque, Field-like torque, MTJ, Switching statistics, Tilted pinned-layer

The magnetic tunnel junction (MTJ) is the basic building block of magnetic random access memory (MRAM) devices. It consists of a thin, nonmagnetic oxide film sandwiched between two magnetic layers. They exhibit tunnel magnetoresistance, where the resistance of the junction depends on the relative orientation of the magnetizations of two magnetic layers. An electric current applies a spin-transfer torque (STT) that tends to align the magnetizations of the magnetic layers.^{1,2} If the direction of the magnetization of one magnetic layer is pinned (fixed), a sufficiently strong STT is able to switch the magnetization of the other (free) layer between two states.³ The spin-transfer torque τ_{STT} due to a spin-polarized current has been phenomenologically described by^{4,5}

$$\tau_{\text{STT}} = a_J \mathbf{m} \times (\mathbf{m} \times \mathbf{m}_p) + b_J \mathbf{m} \times \mathbf{m}_p \quad (1)$$

where the magnetizations of the free and pinned (fixed) layers are denoted by unit vectors \mathbf{m} and \mathbf{m}_p , respectively. The first and second terms of the right-hand side of Eq. (1) are called the Slonczewski and field-like terms, with prefactors a_J and b_J , respectively. The subscript J emphasizes the dependence of these prefactors on the current density J .

The magnetization dynamics is the key factor in designing the switching of high-density scalable STT-MRAM. In particular, one requirement for these devices is that they switch quickly between metastable states. There have been several proposed design strategies to engineer faster switching behavior, such as tilting the magnetization of the pinned-layer away from the easy axis of the free layer⁶⁻⁹ or adding a second polarizer magnet.¹⁰⁻¹² However, these design strategies are typically evaluated assuming that STT is controlled primarily by the Slonczewski-like term in Eq. (1). Experiments have shown that the spin-transfer torque in MTJs also can include a significant field-like term,^{5,13-15} unlike

the case of metallic spin valves.^{16,17} Although b_J can be 10 – 100% of a_J ,^{5,13-15,18,19} the magnitude and sign of b_J is not as well understood as that of a_J ⁵ and the exact bias dependence of b_J is not clear. For example, Sankey *et al.*¹⁴ and Kubota *et al.*¹⁵ found b_J to be quadratic in the bias, while Petit *et al.*¹³ found it to be linear.

Zhou²⁰ obtained theoretical limits for the switching current density and switching time in the presence of the b_J term. Recently Butler *et al.*²¹ applied the Fokker-Planck approach to the switching distributions of spin-torque devices to find the long-time nonswitching (switching) probability for the write (read) process. To do this, they considered the effect of a dimensionless current that lumps together various effects including a_J and b_J . In this work, we use a different approach to study the current-induced switching behavior of a MTJ in the presence of the field-like term with macromagnetic simulations based on a stochastic Landau-Lifshitz-Gilbert equation. In the absence of a field-like term, previous studies have demonstrated the importance of tilting the pinned-layer⁶⁻⁸ and temperature^{22,23} on the switching dynamics; here we consider both of these effects. We also study the switching behavior for the case that b_J is assumed to vary quadratically with J .

We consider the free layer of the MTJ as schematically illustrated in Fig. 1a. The red arrows illustrate \mathbf{m} and \mathbf{m}_p , unit vectors parallel to the magnetization of the free and pinned-layers, respectively. The orientation of \mathbf{m} is described by the polar angle θ and the azimuthal angle ϕ . \mathbf{m}_p is constrained (with no loss of generality) to the xz plane, makes an angle χ with the z axis. We simulate the dynamics of the magnetization of the free layer by integrating the Landau-Lifshitz-Gilbert equation,

$$\frac{d\mathbf{m}}{dt} = -\gamma \mathbf{m} \times \mathbf{H}_{\text{eff}} + \alpha \mathbf{m} \times \frac{d\mathbf{m}}{dt} - \tau_{\text{STT}} \quad (2)$$

where γ is the gyromagnetic ratio, α is the Gilbert damp-

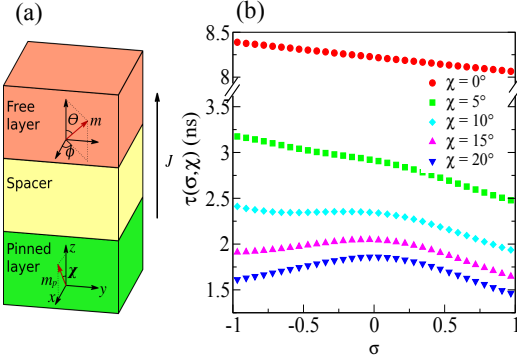


FIG. 1: (a) Schematic illustration of the device studied here. The red arrows show the orientation of the magnetization vectors of the free and pinned-layers. The pinned-layer magnetization is constrained to lie in the x - z plane making an angle χ with the z -axis. (b) Switching time, $\tau(\sigma, \chi)$ as a function of $\sigma = b_J/a_J$ for different values of χ , the tilt angle of the pinned-layer.

ing constant, and \mathbf{H}_{eff} is the effective field. The spin-transfer torque τ_{STT} is described by Eq. (1). We use a convention where $J > 0$ corresponds to electrons moving in the positive direction²⁴ (i.e., the conventional current density has a negative sign when $J > 0$). For the Slonczewski term, we use the standard expression

$$a_J = \frac{\gamma \hbar J \epsilon}{\mu_0 e d M_s} \quad (3)$$

where e , d , and M_s represent the elementary charge, thickness of the free layer, and saturation magnetization, respectively. ϵ characterizes the angular dependence of the Slonczewski term where

$$\epsilon = \frac{P \Lambda^2}{(\Lambda^2 + 1) + (\Lambda^2 - 1)(\mathbf{m} \cdot \mathbf{m}_p)} \quad (4)$$

where P and Λ are dimensionless quantities that determine the spin polarization efficiency.²⁵ We introduce $\sigma = b_J/a_J$ to characterize the relative strength of b_J relative to a_J . We restrict the value of σ from -1 to 1 for all J investigated since experimentally b_J has been found to be 10 – 100% of a_J .^{5,13–15}

For the finite-temperature studies, we augment \mathbf{H}_{eff} with a random fluctuating field \mathbf{H}_r whose statistical properties are given by²⁶ $\langle H_r^i(t) \rangle = 0$ and

$$\langle H_r^i(t) H_r^j(t') \rangle = \frac{2\alpha k_B T}{(1 + \alpha^2) \gamma' M_s \mu_0 V} \delta_{ij} \delta(t - t'), \quad (5)$$

where i and j are Cartesian indices. $\gamma' = \gamma/(1 + \alpha^2)$, V is the volume of the cell, and T is the absolute temperature. $\langle \cdot \cdot \rangle$ denotes the time average of the enclosed quantity.

For all calculations, we set the thickness of the free, spacer, and pinned-layers to 1.3 nm and the cross-sectional area to $100 \times 100 \text{ nm}^2$. The saturation magnetizations for the free and pinned-layers are $M_s =$

1200 kA/m, the uniaxial anisotropy constant $K_u = 2.83 \text{ kJ/m}^3$, the Gilbert damping constant $\alpha = 0.02$, and the spin torque parameters are $P = 0.40$ and $\Lambda = 1$. M_s is consistent with previous reported values for a similar device²⁷. Unless otherwise stated, we set $J = -7.64 \times 10^{10} \text{ A/m}^2$ to fall within the high current limit to ensure switching times of less than 10 ns. The switching time τ is the time for m_z to first change sign.

To understand the switching dynamics, we first perform deterministic 0 K calculations, varying both σ and the pinned-layer tilt angle χ . We note that an average value of θ of 0.01° corresponds to $1 \times 10^{-4} \text{ K}$ using our device parameters after thermal equilibration. Therefore, we set the initial conditions to $\theta = 0.01^\circ$ and $\phi = 0^\circ$. Fig. 1b shows that $\tau(\sigma, \chi)$ generally decreases with increasing χ and $|\sigma|$ except for small χ and negative σ . This can be understood by noting that the field-like term acts as an external field $\mathbf{H}_{\text{FL}} = b_J \mathbf{m}_p / \gamma$, oriented parallel (anti-parallel) to the pinned-layer magnetization for positive (negative) b_J . The effect of \mathbf{H}_{FL} is to create a torque that is proportional to $\sin \theta'$, where θ' is the angle between \mathbf{m} and \mathbf{m}_p , that may move \mathbf{m} out of the easy axis and thus assist in switching. We call this the initial torque effect. \mathbf{H}_{FL} also tends to align \mathbf{m} in the direction of \mathbf{H}_{FL} which may also further assist in switching. We call this the alignment effect. Specifically, we first consider parallel (P) to anti-parallel (AP) switching, which requires $a_J < 0$ (see Fig. 1a). If $\sigma > 0$ then $b_J < 0$ and \mathbf{H}_{FL} is anti-parallel to the pinned-layer magnetization that helps in switching. Thus, both the initial torque and the alignment effect aids P to AP switching. With increasing χ , the initial torque increases and $\tau(\sigma, \chi)$ decreases with χ . Similarly, with increasing σ both the initial torque and alignment effect increases, leading to a decrease in $\tau(\sigma, \chi)$ with σ .

Next, we consider the $\sigma < 0$ case in P to AP switching, where $b_J > 0$ and \mathbf{H}_{FL} is parallel to the fixed layer magnetization. Here, the alignment effect opposes switching. For small χ the initial torque is small and we see an increase in $\tau(\sigma, \chi)$. For large χ , the initial torque may overcome the alignment effect and this may lead to an overall decrease in $\tau(\sigma, \chi)$. The result of $\tau(\sigma, \chi)$ for AP to P switching is exactly the same as that for P to AP since the arguments are the same for both cases. Our analysis suggests that for good P to AP or AP to P switching performance, the sign of b_J should change in such a way that σ is always positive.

We next consider the effect of temperature on switching dynamics using two schemes. In the first, we simulate the system at 0 K so that the trajectories are fully deterministic, but with the initial configurations taken as a result of thermalization at 300 K. This is to provide a better understanding for the second scheme where the simulation is performed at 300 K (non-deterministic trajectories) and the initial configurations are the result of 300 K thermalization. Statistics are collected from 512 identically prepared systems each equilibrated for 60 ns.

In the first scheme, the mean switching time, $\langle \tau_0(\chi) \rangle$

(where the subscript indicates that the switching time is calculated at 0 K) is given by

$$\langle \tau_0(\chi) \rangle = \frac{1}{2\pi} \int_0^{\pi/2} d\theta P(\theta) \sin \theta \int_0^{2\pi} d\phi \tau_0(\theta, \phi, \chi), \quad (6)$$

where $\tau_0(\theta, \phi, \chi)$ denotes the deterministic switching time for an initial spin configuration (θ, ϕ) and a tilt angle χ of the pinned-layer. The equilibrium probability distribution of the magnetization vector \mathbf{m} making an angle θ with the z -axis (averaged over ϕ) $P(\theta) \sin \theta$ (shown in Fig. 2a), accounts for the initial spin configuration at $T = 300$ K and $T = 5$ K. On introducing $\langle \tau_0(\theta, \chi) \rangle_\phi = (2\pi)^{-1} \int_0^{2\pi} d\phi \tau_0(\theta, \phi, \chi)$ as the switching time averaged over ϕ , we reexpress Eq. (6) as

$$\langle \tau_0(\chi) \rangle = \int_0^{\pi/2} d\theta P(\theta) \sin \theta \langle \tau_0(\theta, \chi) \rangle_\phi. \quad (7)$$

Written in this form, the effect of the temperature comes in only through $P(\theta) \sin \theta$, while allowing us to study $\langle \tau_0(\theta, \chi) \rangle_\phi$ which is shown in Fig. 2a for $\chi = 0^\circ$ and $\chi = 20^\circ$ with $\sigma = 0, \pm 1$. First, we consider the case when $\sigma = 0$ (i.e., no field-like term). $\langle \tau_0(\theta, \chi = 0^\circ) \rangle_\phi$ is monotonically decreasing function of θ because initial torque scales as $\sin \theta$. $\langle \tau_0(\theta, \chi = 20^\circ) \rangle_\phi$, however, remains constant for θ from 0 to $\sim 20^\circ$. We note that when θ varies from 0 to $\pi/2$, \mathbf{m} sweeps out progressively larger circles when ϕ changes from 0 to 2π . As shown in Fig. 2b, as θ approaches $\chi = 20^\circ$, some configurations \mathbf{m} may almost align with \mathbf{m}_p that results in a small torque that drastically increases the switching time. However, for other configurations where \mathbf{m} points away from \mathbf{m}_p , the torque increases and the switching time decreases. The overall effect is that the average $\langle \tau_0(\theta, \chi) \rangle_\phi$ is nearly constant from 0 to χ (see Fig. 2a for the case of $\chi = 20^\circ$). The trajectories of \mathbf{m} for $\theta = 17^\circ$ and $\chi = 20^\circ$ for several ϕ values are shown in Fig. 2c which explains a large variation in $\tau_0(\theta, \phi, \chi)$ shown in Fig. 2b for $\theta \approx \chi$.

The mean switching times obtained using Eq. (7) for $\chi = 0^\circ$ and $\chi = 20^\circ$ is 1.75 ns and 1.63 ns, respectively. Thus we see that there is a slight decrease in the mean switching time when χ varies from 0° to 20° . This difference is due to a smaller $\langle \tau_0(\theta, \chi) \rangle_\phi$ for $\chi = 20^\circ$ compared to that for $\chi = 0^\circ$ (see Fig. 2a). Note that the effect of large $\langle \tau_0(\theta, \chi) \rangle_\phi$ difference between $\chi = 0^\circ$ and 20° when θ is small ($< \sim 5^\circ$) as shown in Fig. 2a in determining the mean switching time $\langle \tau_0(\chi) \rangle$ is somewhat suppressed by the small $P(\theta) \sin \theta$ values for these θ at $T = 300$ K.

We now consider the effect of the field-like term in determining the mean switching time. For $\chi = 20^\circ$, $\sigma = 1$ ($\sigma = -1$) leads to a mean switching time of 1.37 ns (1.51 ns); this is smaller than the 1.63 ns time at $\sigma = 0$. When $\chi = 0^\circ$ there is no reduction in the mean switching time in the presence of the field-like term because $\langle \tau_0(\theta, \chi = 0^\circ) \rangle_\phi$ is largely unaffected by the presence of the field-like term (see Fig. 2a) since it does not produce a torque in the z -direction when $\chi = 0^\circ$ for all values of

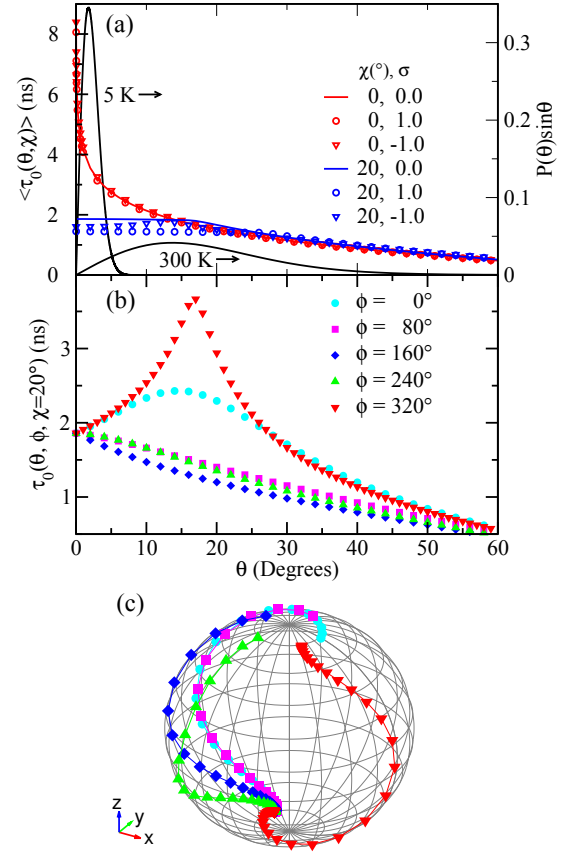


FIG. 2: (a) $\langle \tau_0(\theta, \chi) \rangle_\phi$ versus θ for $\chi = 0^\circ$ and $\chi = 20^\circ$ and $\sigma = 0, \pm 1$. $P(\theta) \sin \theta$ at $T = 300$ K and 5 K are shown as dashed, black lines. (b) $\tau_0(\theta, \phi, \chi = 20^\circ)$ versus θ for several values of ϕ . (c) The trajectories of \mathbf{m} with $\sigma = 0$ and $\theta = 17^\circ$ for several ϕ values. The dots on the trajectories are drawn at equal time intervals. Densely populated dots at the beginning of the $\phi = 320^\circ$ trajectory are due to the small torque in this configuration.

θ and ϕ . We note that $\langle \tau_0(\theta < 0.1^\circ, \chi) \rangle_\phi$ (see Fig. 2a for $\chi = 0^\circ$ and 20° , and $\sigma = 0, \pm 1$) are consistent with the results shown in Fig. 1b.

The switching statistics obtained using the second scheme are shown in Fig. 3a for $T = 300$ K. We find that in the absence of the field-like term, the mean switching times (as deduced from the cumulative distribution probability curve) are 1.71 ns and 1.61 ns for $\chi = 0^\circ$ and $\chi = 20^\circ$, respectively. These are in reasonable agreement with the respective values of 1.75 ns and 1.63 ns obtained using the first scheme. In the presence of the field-like term, the mean switching time remains nearly unchanged compared to the case when the field-like term is absent for $\chi = 0^\circ$. For $\chi = 20^\circ$, the presence of the field-like term with $\sigma = 1$ ($\sigma = -1$) results in mean switching times of 1.35 ns (1.50 ns), which is also consistent with the results obtained in the first scheme. We conclude that temperature changes the switching time mainly through its effect on the initial spin configuration. Since the effect of initial torque is large for large χ , we expect that the

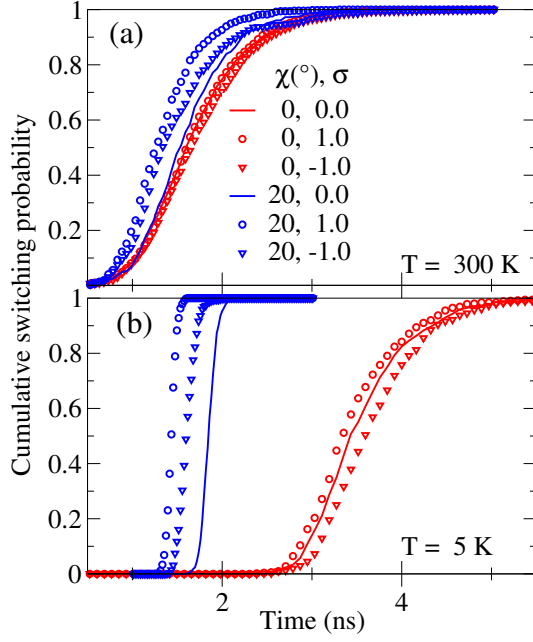


FIG. 3: Cumulative switching probability distributions for $\chi = 0^\circ$ and 20° with $\sigma = 0$ and ± 1 at (a) 300 K and (b) 5 K.

mean switching time will decrease when χ is increased. Indeed, with a typical value of $\chi = 30^\circ$ we find that the mean switching times obtained with the second scheme for $\sigma = 0, 1, -1$ are 1.51, 1.20, and 1.29 ns, respectively. These values are consistently less than the corresponding values for $\chi = 20^\circ$ or $\chi = 0^\circ$.

Similar analysis can also be performed at $T = 5$ K where $P(\theta)\sin\theta$ peaks at small angles ($\sim 2^\circ$). With $\langle\tau_0(\theta, \chi)\rangle_\phi$ (see Fig. 2a), we anticipate that $\chi = 20^\circ$ delivers a much lower mean switching time compared to $\chi = 0^\circ$. Indeed, Fig. 3b shows the mean switching time can be dramatically reduced by tilting the χ from 0° to 20° . Also at $\chi = 20^\circ$, $\sigma = \pm 1$ leads to smaller switching times compared to $\sigma = 0$ since the field-like term introduces a large initial torque.

Finally, we investigate how the switching time changes with current density^{13–15} J when (a) $b_J \propto J$ and (b) $b_J \propto J^2$ for positive (negative) σ in Fig. 4a (Fig. 4b) at $\chi = 10^\circ$. When $b_J \propto J^2$, we work with equivalent expression $b_J = \beta a_J^2$ ($-\beta a_J^2$) and choose β value such that $b_J = 0.5a_J$ ($-0.5a_J$) when $J = 4.0 \times 10^{10}$ A/m² and $b_J = 1.0a_J$ ($-1.0a_J$) when $J = 7.64 \times 10^{10}$ A/m² for $\sigma > 0$ ($\sigma < 0$).

For positive σ both the initial torque as well as the alignment effect aid in switching; therefore, we see a reduction in the switching time for all J . Since with increasing magnitude of σ , both the effects increase, we see larger reduction in the switching time for larger $\sigma = 1$, i.e., $b_J = a_J$ compared to smaller $\sigma = 0.5$. Also, when b_J varies quadratically with J , the switching time decreases more rapidly with J compared to the case when b_J has linear dependence on J . This rapid decrease results from

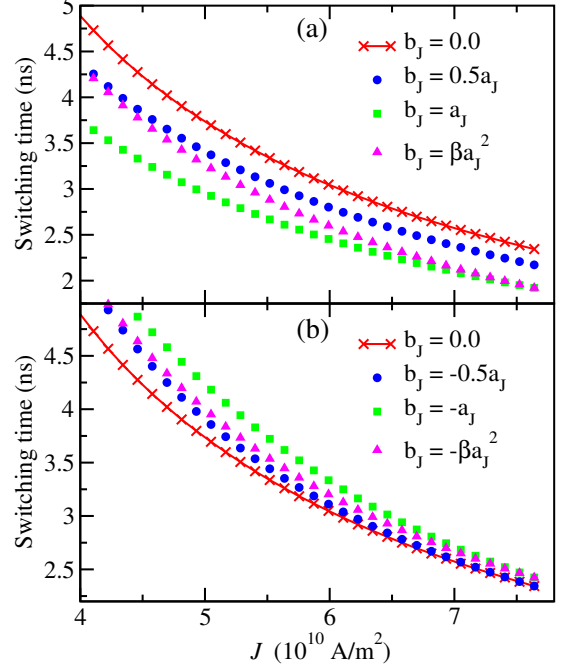


FIG. 4: Variation of the switching time with the current density J when $b_J \propto J$ and $b_J \propto J^2$ for (a) positive σ and (b) negative σ .

increasing σ with increasing J for the quadratic dependence.

For negative σ , we see that there is, in fact, an increase in the switching time in the presence of the field-like term. This is attributable to the alignment effect (which opposes switching) dominating the initial torque effect. Also, with increasing σ , the alignment effect increases more rapidly compared to the initial torque effect. As a result we see longer switching time for $\sigma = -1$, i.e., $b_J = -a_J$ compared to that of $\sigma = -0.5$, i.e., $b_J = -0.5a_J$. For the quadratic dependence b_J on J , the rate of the switching time increase with J compared to that of linear dependence because increase in J leads to increased σ . Thus we see that the field-like term may improve the switching time if b_J changes sign the same way as the a_J changes and a quadratic dependence of b_J with J could lead to a larger reduction as compared with the linear case.

In summary, we have employed the Landau-Lifshitz-Gilbert equation to simulate the behavior of a MTJ with a tilted pinned-layer at finite temperatures, taking the field-like term into account. The field-like spin-transfer torque b_J is important to the switching dynamics only if the pinned-layer is tilted. Our simulations illustrate the simultaneous effect of geometry and the field-like term on switching distributions at finite temperatures. The present results should allow for a more science-based engineering of MTJ switching performance.

-
- * Electronic address: ganck@ihpc.a-star.edu.sg
- ¹ J. C. Slonczewski, J. Magn. Magn. Mater. **159**, L1 (1996).
 - ² L. Berger, Phys. Rev. B **54**, 9353 (1996).
 - ³ E. B. Myers, D. C. Ralph, J. A. Katine, R. N. Louie, and R. A. Buhrman, Science **285**, 867 (1999).
 - ⁴ O. G. Heinonen, S. W. Stokes, and J. Y. Yi, Phys. Rev. Lett. **105**, 066602 (2010).
 - ⁵ Z. Li, S. Zhang, Z. Diao, Y. Ding, X. Tang, D. M. Apalkov, Z. Yang, K. Kawabata, and Y. Huai, Phys. Rev. Lett. **100**, 246602 (2008).
 - ⁶ X. Zhu and J. Zhu, IEEE Trans. Magn. **42**, 2739 (2006).
 - ⁷ Y. Zhou, C. L. Zha, S. Bonetti, J. Persson, and J. Åkerman, Appl. Phys. Lett. **92**, 262508 (2008).
 - ⁸ Y. Zhou, C. L. Zha, S. Bonetti, J. Persson, and J. Åkerman, J. Appl. Phys. **105**, 07D116 (2009).
 - ⁹ Y. Zhou, S. Bonetti, C. L. Zha, and J. Åkerman, New J. Phys. **11**, 103028 (2009).
 - ¹⁰ A. Kent, B. Özyilmaz, and E. Del Barco, Appl. Phys. Lett. **84**, 3897 (2004).
 - ¹¹ R. Sbiaa, R. Law, E. Tan, and T. Liew, J. Appl. Phys. **105**, 013910 (2009).
 - ¹² Z. Diao, A. Panchula, Y. Ding, M. Pakala, S. Wang, Z. Li, D. Apalkov, H. Nagai, A. Driskill-Smith, L. Wang, *et al.*, Appl. Phys. Lett. **90**, 132508 (2007).
 - ¹³ S. Petit, C. Baraduc, C. Thirion, U. Ebels, Y. Liu, M. Li, P. Wang, and B. Dieny, Phys. Rev. Lett. **98**, 077203 (2007).
 - ¹⁴ J. C. Sankey, Y. T. Cui, J. Z. Sun, J. C. Slonczewski, R. A. Buhrman, and D. C. Ralph, Nat. Phys. **4**, 67 (2008).
 - ¹⁵ H. Kubota, A. Fukushima, K. Yakushiji, T. Nagahama, S. Yuasa, K. Ando, H. Maehara, Y. Nagamine, K. Tsunekawa, D. Djayaprawira, N. Watanabe, and Y. Suzuki, Nat. Phys. **4**, 37 (2008).
 - ¹⁶ K. Xia, P. J. Kelly, G. E. W. Bauer, A. Brataas, and I. Turek, Phys. Rev. B **65**, 220401 (2002).
 - ¹⁷ M. A. Zimmler, B. Özyilmaz, W. Chen, A. D. Kent, J. Z. Sun, M. J. Rooks, and R. H. Koch, Phys. Rev. B **70**, 184438 (2004).
 - ¹⁸ I. Theodonis, N. Kioussis, A. Kalitsov, M. Chshiev, and W. Butler, Phys. Rev. Lett. **97**, 237205 (2006).
 - ¹⁹ J. C. Slonczewski and J. Z. Sun, J. Magn. Magn. Mater. **310**, 169 (2007).
 - ²⁰ Y. Zhou, J. Appl. Phys. **109**, 023916 (2011).
 - ²¹ W. H. Butler, T. Mewes, C. K. A. Mewes, P. B. Visscher, W. H. Rippard, S. E. Russek, and R. Heindl, IEEE Trans. Magn. **48**, 4684 (2012).
 - ²² Z. Diao, Z. Li, S. Wang, Y. Ding, A. Panchula, E. Chen, L. Wang, and Y. Huai, J. Phys.: Condens. Matter **19**, 165209 (2007).
 - ²³ P. M. Braganca, I. N. Krivorotov, O. Ozatay, A. G. F. Garcia, N. C. Emley, J. C. Sankey, D. C. Ralph, and R. A. Buhrman, Appl. Phys. Lett. **87**, 112507 (2005).
 - ²⁴ Z. H. Xiao, X. Q. Ma, P. P. Wu, J. X. Zhang, L. Q. Chen, and S. Q. Shi, J. Appl. Phys. **102**, 093907 (2007).
 - ²⁵ J. Xiao, A. Zangwill, and M. D. Stiles, Phys. Rev. B **70**, 172405 (2004).
 - ²⁶ J. L. García-Palacios and F. J. Lázaro, Phys. Rev. B **58**, 14937 (1998).
 - ²⁷ S. Ikeda, K. Miura, H. Yamamoto, K. Mizunuma, H. D. Gan, M. Endo, S. Kanai, J. Hayakawa, F. Matsukura, and H. Ohno, Nature Materials **9**, 721 (2010).